Geophysical Research Letters

RESEARCH LETTER
10.1029/2024GL109369

Reactive Nitrogen Partitioning Enhances the Contribution of Canadian Wildfire Plumes to US Ozone Air Quality

Meiyun Lin[1], Larry W. Horowitz[1], Lu Hu[2], and Wade Permar[2]

[1]NOAA Geophysical Fluid Dynamics Laboratory, Princeton, NJ, USA, [2]Department of Chemistry and Biochemistry, University of Montana, Missoula, MT, USA

Key Points:

- Sequestration of wildfire NO_x emissions in Canada as peroxyacetyl nitrate (PAN) enhances the downwind impacts on US O_3 air quality
- Pyrogenic volatile organic compounds and PAN decomposition increase the contribution of aged Canadian smoke plumes to O_3 in US cities
- Accounting for these effects in a high-resolution chemistry-climate model improves simulation of smoke-impacted high-O_3 events in US cities

Supporting Information:

Supporting Information may be found in the online version of this article.

Correspondence to:

M. Lin,
Meiyun.Lin@noaa.gov

Citation:

Lin, M., Horowitz, L. W., Hu, L., & Permar, W. (2024). Reactive nitrogen partitioning enhances the contribution of Canadian wildfire plumes to US ozone air quality. *Geophysical Research Letters*, *51*, e2024GL109369. https://doi.org/10.1029/2024GL109369

Received 1 APR 2024
Accepted 2 JUL 2024

Author Contributions:

Conceptualization: Meiyun Lin
Data curation: Lu Hu, Wade Permar
Formal analysis: Meiyun Lin
Methodology: Meiyun Lin
Software: Meiyun Lin
Validation: Meiyun Lin, Larry W. Horowitz
Writing – original draft: Meiyun Lin
Writing – review & editing: Meiyun Lin, Larry W. Horowitz

Abstract Quantifying the variable impacts of wildfire smoke on ozone air quality is challenging. Here we use airborne measurements from the 2018 Western Wildfire Experiment for Cloud Chemistry, Aerosol Absorption, and Nitrogen (WE-CAN) to parameterize emissions of reactive nitrogen (NO_y) from wildfires into peroxyacetyl nitrate (PAN; 37%), NO_3^- (27%), and NO (36%) in a global chemistry-climate model with 13 km spatial resolution over the contiguous US. The NO_y partitioning, compared with emitting all NO_y as NO, reduces model ozone bias in near-fire smoke plumes sampled by the aircraft and enhances ozone downwind by 5–10 ppbv when Canadian smoke plumes travel to Washington, Utah, Colorado, and Texas. Using multi-platform observations, we identify the smoke-influenced days with daily maximum 8-hr average (MDA8) ozone of 70–88 ppbv in Kennewick, Salt Lake City, Denver and Dallas. On these days, wildfire smoke enhanced MDA8 ozone by 5–25 ppbv, through ozone produced remotely during plume transport and locally via interactions of smoke plume with urban emissions.

Plain Language Summary Wildfires have torn across western North America over the last decade. Smoke from wildland fires in Canada can travel thousands of kilometers to US cities and reacts with urban pollution to create harmful ozone, a criteria pollutant regulated by the US Environmental Protection Agency. Accurately quantifying this impact is needed to inform US air quality policy, but is challenging due to complex physical and chemical processes. In this study, we analyze surface and airborne measurements, alongside a new variable-resolution global chemistry-climate model, to better understand these processes. We show that the near-field conversion of nitrogen oxide (NO_x) emissions from wildfires to peroxyacetyl nitrate (PAN) and other more oxidized forms reduces their localized impacts on ozone. PAN is the principal tropospheric reservoir for NO_x radicals. When aged smoke plumes descend southward from Canada toward US cities, higher temperatures cause PAN to decompose and thus help production of ozone during smoke transport. On days when the observed ozone levels exceed the air quality limit (70 ppbv for 8-hr average), wildfire smoke can contribute 5–25 ppbv.

1. Introduction

Large wildfires have become increasingly common during recent decades in Canada, the Pacific Northwest, and California, causing severe air pollution, loss of human life, and property damage (Abatzoglou & Williams, 2016; Brown et al., 2023). Five of the most destructive wildfire seasons of the last half-century occurred in the past 7 years: 2017, 2018, 2020, 2021, and 2023, raising the possibility that climate change is already driving changes in fire regimes (Hagmann et al., 2021; Parisien et al., 2023; Xie et al., 2020, 2022). Biomass burning (BB) in wildfires emits particulate matter along with hundreds of reactive gases, including nitrogen oxides (NO_x), nitrous acid (HONO), carbon monoxide (CO), ammonia (NH_3), and an enormous diversity of volatile organic compounds (VOCs) (Coggon et al., 2019; Hatch et al., 2017; Liang et al., 2022; Permar et al., 2021). The complex chemical cocktail of wildfire smoke presents challenges for understanding fire impacts on secondary air pollutants such as ozone (O_3) (Jaffe et al., 2020).

Wildfire emissions have variable impacts on O_3. O_3 is usually enhanced downwind from wildfire plumes with moderate smoke levels, and the O_3 production increases with plume age (Jaffe & Wigder, 2012). At high smoke levels, O_3 formation is suppressed, in part due to low-light conditions or heterogeneous chemistry on smoke particles (e.g., Alvarado et al., 2015; Palm et al., 2021). Observations show that emissions of HONO and NO_x in boreal and temperate smoke plumes are rapidly (within minutes to a few hours after emissions) converted into peroxyacyl nitrates (PANs) and particulate nitrate (pNO_3), such that O_3 production in wildfire plumes rapidly becomes NO_x-limited (Alvarado et al., 2010; Juncosa Calahorrano et al., 2021; Xu et al., 2021). The lifetime of

NO_x is approximately 1 day, while the lifetime of PAN in the mid-troposphere is at least a month (Jacob, 1999). Once ventilated from a source region to the cold free-troposphere where it is more stable, PAN can be efficiently transported on hemispheric scales (Fiore et al., 2018; Fischer et al., 2014; Lin et al., 2010;). When a smoke plume subsides, PAN thermally decomposes to release NO_x, thus facilitating O_3 formation far downwind (Bourgeois et al., 2021; Liu et al., 2016). O_3 produced during smoke transport appears to be the main driver of O_3 increases in NO_x-sensitive urban areas (Langford et al., 2023; Rickly et al., 2023). Injection of VOC-rich smoke plumes into NO_x-rich urban areas can enhance O_3 production additionally (e.g., McClure and Jaffe, 2018; Pan & Faloona, 2022).

Modeling large fire-to-fire variations in emission factors, smoke physics, plume dynamics and chemical evolution is challenging (Jaffe et al., 2020; L. Jin et al., 2023; Ye et al., 2021). Current chemical transport models (with horizontal resolution of 4–200 km) typically overestimate O_3 close to fires, while having difficulty simulating the long-range influence of aged smoke plumes on downwind O_3 (Baker et al., 2016, 2018; Bourgeois et al., 2021; Fiore et al., 2014; Singh et al., 2012; Tang et al., 2022; Zhang et al., 2014, 2020). Large uncertainties exist in the partitioning of reactive nitrogen (NO_y), with models typically underestimating organic nitrates and PANs in smoke (Arnold et al., 2015; Cai et al., 2016). The 2018 Western Wildfire Experiment for Cloud Chemistry, Aerosol Absorption, and Nitrogen (WE-CAN) and other recent aircraft field campaigns systematically sampled the first few hours of chemical evolution in wildfire plumes, critical for evaluating and improving models (Juncosa Calahorrano et al., 2021; Lindaas et al., 2021b; Permar et al., 2021; Warneke et al., 2023).

Here we use WE-CAN airborne measurements to partition wildfire NO_y emissions into NO_x, PAN, and NO_3^- ($NO_3^- = HNO_3 + pNO_3$) in a variable-resolution global chemistry-climate model (AM4VR) (Lin et al., 2024). We show that sequestration of wildfire NO_x emissions in the Pacific Northwest as PAN enhances their downwind impacts on O_3 in US cities designated as O_3 nonattainment areas, including Salt Lake City, Denver and Dallas (US EPA, 2024). With regional grid refinements providing 13 km resolution over the contiguous US, AM4VR allows us to investigate interactions between urban pollution and smoke plumes from fires thousands of kilometers away. We assess the contribution of these interactions to the observed high-O_3 episodes by analyzing a suite of model simulations alongside satellite images, aircraft sampling of smoke plumes, and ground-based measurements.

2. Observations and Identification of Smoke-Influenced High-O_3 Days

The buildup of O_3 produced from urban emissions under hot and dry meteorological conditions can complicate the attribution of observed O_3 enhancements to smoke influence (Lin et al., 2017, 2020; Lindaas et al., 2017). We identify high-O_3 episodes in Colorado and Texas influenced by Canadian wildfire smoke, using these criteria: (a) Satellite observations show enhancements of aerosol optical depth across the Great Plains and animation of the Geostationary Operational Environmental Satellite (GEOS) natural-color images (https://star.nesdis.noaa.gov/smcd/spb/aq/AerosolWatch/) shows passage of a cold front toward the Southern Great Plains; (b) Ground sites in Colorado and Texas record $PM_{2.5}$ greater than 35 μg/m^3 for 24-hr mean; (c) IMPROVE ground sites measure enhancements (+50% above background) in organic aerosol (OA), a key component of wildfire smoke (Garofalo et al., 2019); and (d) Ground sites measure surface O_3 above the 70 ppbv National Ambient Air Quality Standard for daily maximum 8-hr average (MDA8).

Applying these criteria for 2018, we identify smoke-influenced high-O_3 days in the Colorado Front Range Urban Corridor on 20 and 24 August, and in the US Deep South on 20–21 August (Figure 1). On 19–20 August, GOES and surface observations showed heavy smoke from wildfires burning in British Columbia and other areas in the Pacific Northwest (Figures 1a–1d). A cold front passed across the Great Plains, transporting wildfire smoke toward the US Deep South (Figure 1b). Surface $PM_{2.5}$ of 30–60 μg/m^3 were observed on 20–21 August at sites across the Colorado Front Range Urban Corridor to Amarillo and Dallas, Texas, where background $PM_{2.5}$ were <10 μg/m^3 (Figures 1c–1f). The IMPROVE Wichita Mountains monitor located close to the Oklahoma-Texas border, showed increased OA on 21 August, supporting the smoke influence in this region. Surface MDA8 O_3 of 70–88 ppbv was observed at monitors along the smoke transport pathway across Colorado to Texas on 20–21 August. During 23–24 August, a new cold front transported smoke across the western US, elevating MDA8 O_3, $PM_{2.5}$ and OA in Colorado, but this cold front did not propagate toward Texas. In contrast to the O_3 episodes associated with in-situ production from anthropogenic emissions (e.g., 1–3 August), the smoke-impacted periods exhibit a chemical signature with enhancements in OA.

10.1029/2024GL109369

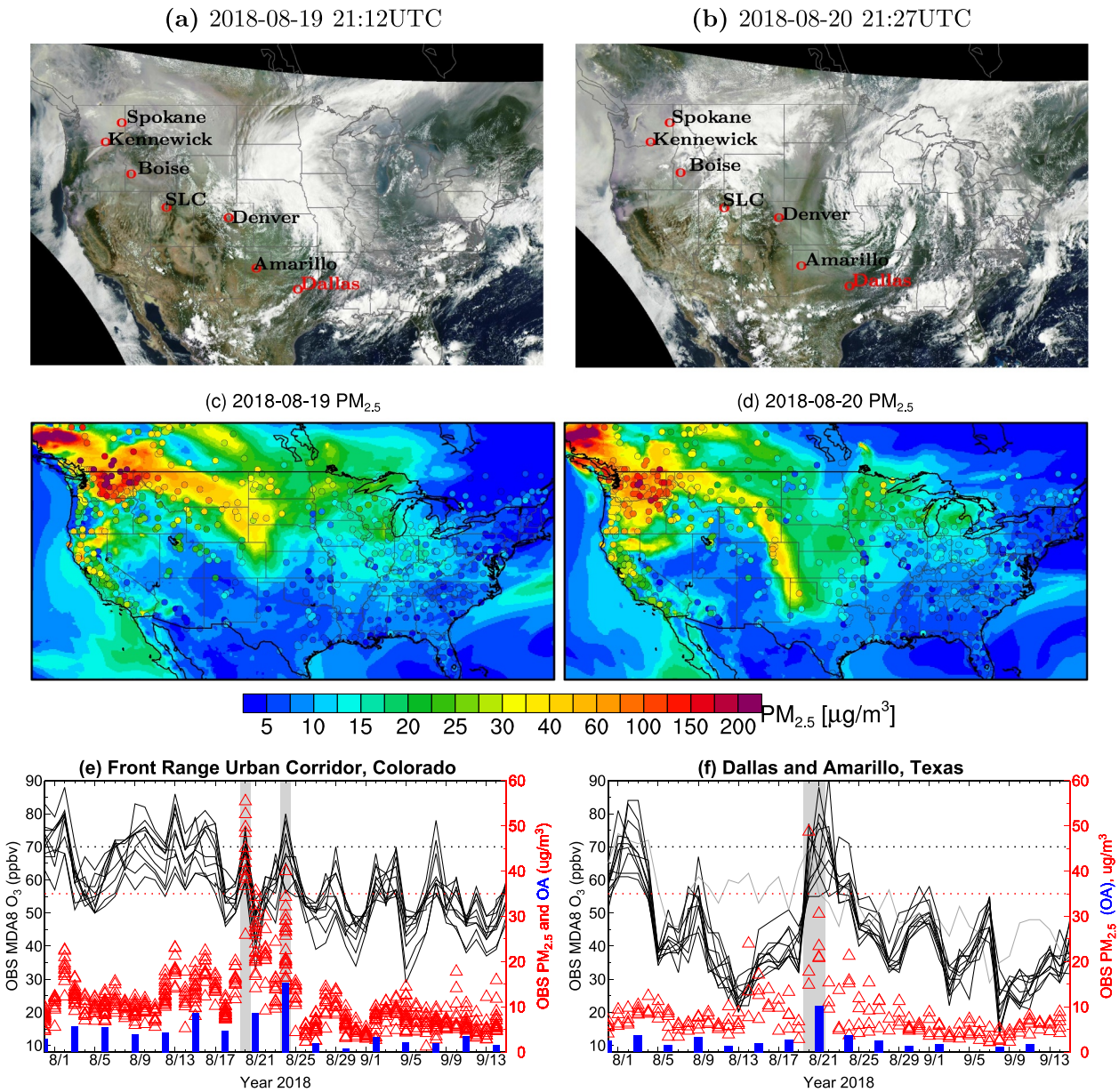

Figure 1. (a, b) GOES natural-color images on 19 and 20 August 2018. Cities referenced in the article are labeled. (c, d) Observed (circles) and simulated (shading) surface $PM_{2.5}$ concentrations. (e, f) Time series of observed daily MDA8 O_3 (black lines) and $PM_{2.5}$ (red triangles) at sites in the Front Range Urban Corridor, Colorado and in Dallas (black) and Amarillo (gray), Texas. Blue bars show organic aerosol (OA) measured by IMPROVE every 3 days at Rocky Mountain, Colorado and Wichita Mountains, Oklahoma.

3. Model Simulations

AM4VR is a new variable-resolution global chemistry-climate model developed at NOAA's Geophysical Fluid Dynamics Laboratory for research at the nexus of US climate and air quality extremes (Lin et al., 2024). For this study, we conduct nudged AM4VR simulations for 2018 using daily emissions from the Global Fire Emission Database (0.25° × 0.25°) (van der Werf et al., 2017), distributed vertically between the surface and 6 km based on an injection height climatology from satellite-based Multi-angle Imaging SpectroRadiometer (MISR) (Val Martin et al., 2018). AM4VR includes a revised treatment of VOC emissions, accounting for emissions of acetaldehyde (CH_3CHO) and methyl ethyl ketone (MEK, C_4H_8O), both precursors of PAN, from wildfires that are ignored in our previous model AM4.1.

Four AM4VR model experiments are designed to explore the impacts of oxygenated VOC (OVOC) emissions and NO_y evolution in wildfire smoke (Table S1 in Supporting Information S1). Fires in our BASE model emit NO_y purely as NO, similar to previous models. Juncosa Calahorrano et al. (2021) showed that, within a few hours after emissions, approximately 37% of the total NO_y species is PANs, with pNO_3 the second largest contributor (27%), based on data averaged over all fresh plume transects during WE-CAN. Since our model does not fully resolve the rapid chemical transformations within concentrated smoke plumes, we thus parameterize NO_y fire emissions as 37% PAN, 27% HNO_3, and 36% NO in a second simulation (hereafter AM4VR), as in Lin et al. (2024). Gas-phase HNO_3 and pNO_3 are re-equilibrated each timestep depending on temperature and NH_3 availability (Fountoukis & Nenes, 2007; Lindass et al., 2021a). We conduct two additional simulations: one with BB emissions of OVOCs (HCHO, CH_3CHO, and CH_3COCH_3) increased by a factor of 2 (hereafter OVOCx2; NO_y emissions treated as in BASE), and the other with emissions of NO_y, VOCs, and other gases from fires zeroed out (hereafter noBB).

The average $\Delta PAN/\Delta NO_y$ ratio derived from WE-CAN (37%) is within the 30%–40% range from other field studies of temperate and boreal fires (Table S2 in Supporting Information S1; Alvarado et al., 2010; Liu et al., 2016; Xu et al., 2021). Thus, our parametrization approach is applicable to other years, although it does not capture fire-to-fire variability (e.g., fires with colder conditions have a higher VOC-to-NO_x emission ratio, favoring PAN formation). As we have more detailed near-field measurements in the future, geographically varying, biome-dependent NO_y partitioning can be explored. The approach may be implemented in a similar way as to how parameterizations have been previously adopted for aircraft and shipping NO_x emissions (e.g., Cariolle et al., 2009).

4. Rapid NO_y Evolution Slows Ozone Formation in Near-Fire Smoke Plumes

We first assess the impacts of NO_y partitioning on O_3 formation in the near-fire (<1 day of aging) western US smoke plumes sampled by WE-CAN in summer 2018 (Text S1 and Figure S1 in Supporting Information S1). The BASE model, with fires emitting NO_y purely as NO, captures up to ∼50% of the observed PAN abundance and generally overestimates O_3 in fresh wildfire smoke (Figure 2). Comparisons of CO, HCHO, CH_3CHO, and CH_3COCH_3 indicate underestimates of simulated VOCs in smoke, likely resulting from too low primary emissions, missing secondary production pathways, and non-implemented VOCs, thus contributing to the underestimate of PAN (Text S2 and Figure S2 in Supporting Information S1). In addition, numerical dilution of smoke plumes into large model grid boxes presents challenges for our model, even with 13 km resolution, to capture rapid photochemical processes that occur in a concentrated smoke plume within minutes after emissions. Supporting these statements, we find that doubling OVOC emissions from fires favors PAN formation by producing more acetyl peroxy radical (CH_3CO_3), but is insufficient to remove the bias. Using the empirical partitioning of NO_y emissions from fires including PAN and NO_3^- thus accounts for additional VOC emissions and rapid chemistry in smoke.

With NO_y partitioning, the regression slope of simulated PAN with WE-CAN observations increases from 0.51 to 0.73 (Figure 2a). The overall root-mean-square-error (rmse) decreases from 160 to 97 pptv. Rapid conversion of NO_x to PAN and NO_3^- reduces excessive O_3 production simulated in near-fire smoke plumes, decreasing the overall rmse from 11 to 7 ppbv (Figure 2b). O_3 decreases by 10–23 ppbv in the fresh smoke plumes sampled on 26 July and 2, 8, 9, and 13 August. On 13 August, the aircraft sampled smoke from wildfires in the Salmon Challis National Forest in Idaho (Figure S1 in Supporting Information S1). Intercepted at ∼4.5 km altitude between 22:00–23:30 UTC, this smoke plume exhibits factors of 2–5 times enhancements of PAN above its background level (Figure 2c). On 2 August, the aircraft intercepted fresh plumes from fires burning in Southwest Oregon. With NO_y partitioning, AM4VR captures the observed in-plume PAN abundance approaching 3–8 ppbv (Figures 2c and 2d). In contrast, BASE captures less than 30% of observed PAN levels. The NO_x loss to NO_3^- and PAN decreases MDA8 O_3 by ∼15 ppb in surface air over the burned area around the Idaho/Montana border (Figure 3a). The lower O_3 simulated by AM4VR agrees well with WE-CAN observations (Figure 3c). AM4VR also captures the observed MDA8 O_3 exceedances in Salt Lake City influenced by aged smoke (Figure 3a and Figure S3 in Supporting Information S1).

On 26 July, the aircraft sampled smoke from the Carr Fire in the wildland-urban interface of northern California (Figure 3b). PAN was not measured on this flight. The smoke plume over northern California exhibited O_3 mixing

10.1029/2024GL109369

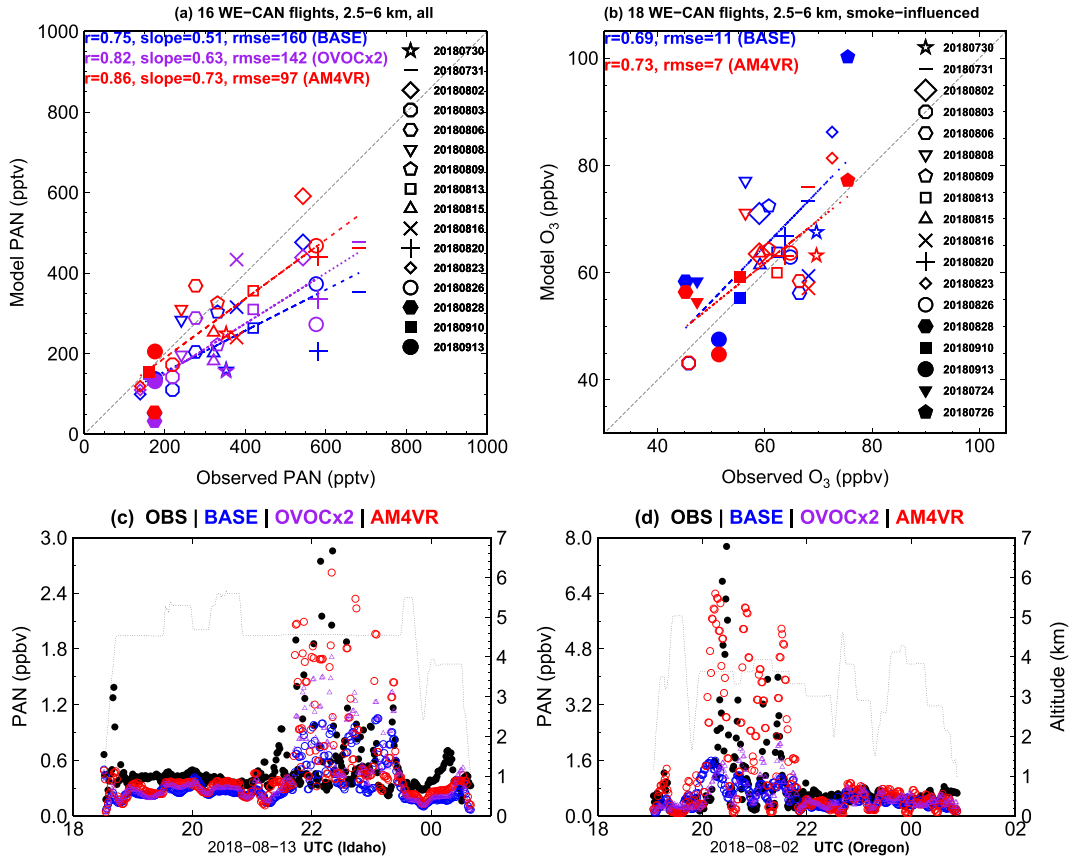

Figure 2. (a) Scatter plots of observed and simulated median mixing ratios of peroxyacetyl nitrate (PAN) during the Western Wildfire Experiment for Cloud Chemistry, Aerosol Absorption, and Nitrogen (WE-CAN): each dot represents average of all data between 2.5 and 6 km altitude for each flight. Results are shown for BASE with Biomass burning (BB) emitting NO_y as 100% NO (blue), for doubling fire oxygenated volatile organic compound (OVOC) emissions (purple), and for AM4VR (red) with BB emitting NO (36%), HNO_3 (27%), and PAN (37%); (b) Same as (a) but for median O_3 in smoke-influenced environments (observed CO > 85 ppbv, HCN > 275 pptv, and CH_3CN > 200 pptv); (c, d) Comparison of observed and simulated PAN for 13 and 2 August flights (dotted lines denote flight altitude).

ratios of 85–120 ppbv at ∼4 km altitude, compared to ∼65 ppbv in the remote Idaho plume (Figure 3d). Fires burning in close proximity to NO_x-rich urban areas in California had a greater impact on O_3 formation. AM4VR represents the vertical structure of the smoke plume and the observed magnitude of O_3. The NO_y parameterization reduces free tropospheric O_3 by ∼23 ppbv in smoke-influenced environments (blue vs. red pentagons in Figure 2b). This is consistent with box modeling suggesting that O_3 formation in VOC-rich smoke plumes is mostly NO_x-limited (X. Jin et al., 2023; Xu et al., 2021).

AM4VR captures the large-scale structure of smoke plumes compared with aircraft observations. WE-CAN sampled plumes between 2 and 5 p.m. (local time) when fires are active and plumes are injected high in the atmosphere. The injection height derived from MISR with a 10:30 a.m. overpass is biased low. The simulated vertical distribution of tracers in smoke plumes is not only determined by the MISR injection height climatology but also by strong vertical mixing under hot meteorological conditions. There are cases in which we identified model PAN biases caused by insufficient injection height. On 30 July (stars in Figures 2a and 2b), for example, the aircraft intercepted fresh smoke plumes at 3–4 km altitude, while the model simulated plumes at ∼2 km altitude (Figure S4 in Supporting Information S1). Despite this bias in altitude, the NO_y partitioning consistently leads to enhanced PAN and reduced O_3 in the simulated fresh plumes.

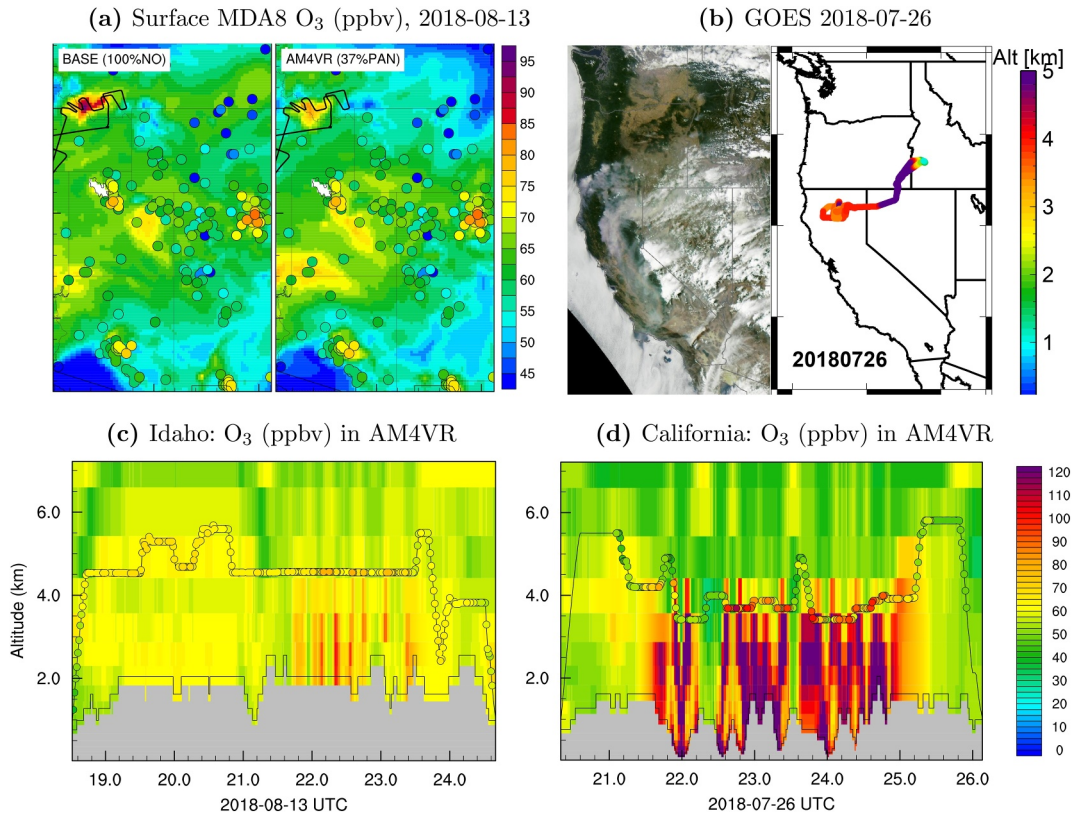

Figure 3. (a) Maps of surface MDA8 O_3 on 13 August from BASE (left) and AM4VR (right) simulations, with color-coded circles representing observations and black lines showing flight track. (b) GOES natural-color image and flight track on 26 July. (c, d) Observed (circles) and AM4VR simulated O_3 for 13 August and 26 July flights.

5. Ozone Formation in Aged Wildfire Smoke

We next examine the impact of aged wildfire smoke on urban O_3 air quality, following long-range transport over thousands of kilometers. We focus on the 16–24 August period when several cold fronts transported smoke from numerous fires burning in the Pacific Northwest to Kennewick, Salt Lake City, Denver, and the US Deep South (Figure S5 in Supporting Information S1). Comparisons of surface MDA8 O_3 from observations and model sensitivity experiments demonstrate the role of NO_x supply from urban pollution and PAN decomposition on O_3 formation in VOC-rich smoke plumes (Table 1).

Over Washington state, enhancements of O_3 in wildfire smoke were greatest on 16 and 22 August when smoke levels were moderate ($PM_{2.5}$ = 30–60 μg/m^3, Text S3 in Supporting Information S1). Observed MDA8 O_3 is 80 ppbv at Spokane and 86 ppbv at Kennewick on 16 August (Figure 4a). Simulated O_3 is below 60 ppbv in noBB, indicating minor influence of O_3 produced from local anthropogenic emissions alone. Accounting for emissions from fires, simulated O_3 increases to 72–74 ppbv in BASE, still lower than observed. When NO_y emissions partitioning is included, more PAN is formed in fresh plumes and subsequently decomposes during smoke transport, enhancing downwind O_3 formation and increasing simulated MDA8 O_3 to 78 ppbv at Spokane and Kennewick. Similarly, NO_y parametrization enhances MDA8 O_3 by 7–11 ppbv on 22 August, leading to better agreement of simulated O_3 with observations (Table 1). The enhancement due to NO_y parametrization occurs broadly upwind of the urban areas, indicating that O_3 was primarily produced within the smoke and transported into the Tri-Cities airshed (Movies S1 and S2).

Over the Colorado Front Range and Texas, observations show elevated MDA8 O_3 of 70–88 ppbv in Denver, Amarillo and Dallas during 20–21 August (Figure 4b and Table 1). In these areas, O_3 was enhanced by production during smoke transport plus the in-situ production from mixing of smoke VOCs with urban NO_x. As smoke descended toward the US Deep South and warmed in the dry air stream of the

Table 1
Observed and Simulated MDA8 O_3 (ppbv) at Western US Cities Influenced by Aged Wildfire Smoke in August 2018

Date	Location	OBS	noBB	BASE	AM4VR	AM4VR—noBB (total smoke impact)	AM4VR—BASE (impact of NO_y parameterization)
August 16	Spokane	80	59	74	78	19	4 (21%)
	Kennewick	86	54	72	78	24	6 (25%)
August 20	Denver/Boulder (5 sites)	69–74	50–60	61–66	68–74[a]	15–24	5–8 (30%)
	Amarillo	71	41	56	65	24	9 (37%)
	Dallas (3 sites)	73–78	60–66	60–66	68–73	10–18	5–12 (50%)
August 21[b]	Dallas (4 sites)	75–88	65–70	70–78	70–75	5–8	N.A.
August 22	Spokane	68	46	60	67	21	7 (33%)
	Kennewick	73	46	60	71	25	11 (44%)
	Portland	75	50	62	70	20	8 (40%)
August 23	Salt Lake City (4 sites)	67–77	50–55	65–75	65–78	15–20	4 (<20%)
August 24[b]	Denver/Boulder (5 sites)	70–80	50–58	69–73	67–72	10–15	N.A.

[a]Model does not resolve site-to-site O_3 variations in cities. The range of simulated values in the area is reported. [b]N.A. indicates cases where NO_y emission partitioning has little impact on simulated urban O_3.

cold front (Figure 1b), PAN decomposed to release NO_x and thus facilitated O_3 formation during smoke transport. Supporting this conclusion, AM4VR with NO_y parameterization simulates well the observed O_3 levels in Denver–Boulder and Dallas on 20 August, increasing MDA8 O_3 by 5–12 ppbv relative to BASE and 10–24 ppbv relative to noBB (see also Figure S6 in Supporting Information S1). The NO_y parameterization accounts for ∼30% of the total MDA8 O_3 enhancement due to imported smoke in Denver. Observed O_3 was highest along the foothills west of downtown Denver, suggesting additional O_3 production from reactions of smoke VOCs with urban NO_x. In Amarillo and Dallas, O_3 produced during smoke transport is the main driver for O_3 increases on 20 August, as evidenced from the significant impact of NO_y parameterization (∼50%). During 21 August, as smoke further mixed into surface air in Dallas, NO_y parameterization shows little impact on simulated O_3, implying that urban pollution provided critical NO_x for O_3 production. Interaction of pyrogenic VOCs with urban NO_x in Dallas increased MDA8 O_3 by 5–8 ppbv on 21 August (BASE—noBB in Table 1).

During 23–24 August, a new cold front transported smoke toward Salt Lake City and Denver (Figure 5). Smoke plumes were intercepted by the aircraft below ∼4 km during the ascent from Boise, between 1 and 3 km off the California coast, and below ∼4 km during the descent to Boise (Figures 5a and 5b). The estimated chemical age is 1–3 days for the plumes over Boise and >3 days for the plume off the California coast (O'Dell et al., 2020; Permar et al., 2023). These aged smoke plumes exhibit lower PAN and higher O_3 levels compared to the fresh plumes sampled by WE-CAN (Figure 2). The plume off the California coast exhibits O_3 above 100 ppbv and PAN below 0.5 ppbv. AM4VR with NO_y parameterization better captures enhancements of O_3 with increased plume age, compared with BASE (Figure 5b vs. Figure 5d).

As the smoke plumes mixed with urban pollution across the western US, observations show MDA8 O_3 increased by 10–20 ppbv in Salt Lake City on 23 August and in the Denver-Boulder area on 24 August relative to 22 August (Figure 5e). AM4VR captures the observed features, simulating increased O_3 in the descending dry air stream of the cold front. Without BB emissions of VOCs and NO_y, simulated O_3 decreased in Salt Lake City on 23 August and in Denver on 24 August, indicating that the cold front would otherwise transport clean air to these areas (Figure 5f). Over Oklahoma and northern Texas, noBB showed enhanced MDA8 O_3 on 23–24 August, indicating that the O_3 pollution was primarily produced from regional anthropogenic emissions. This attribution is consistent

10.1029/2024GL109369

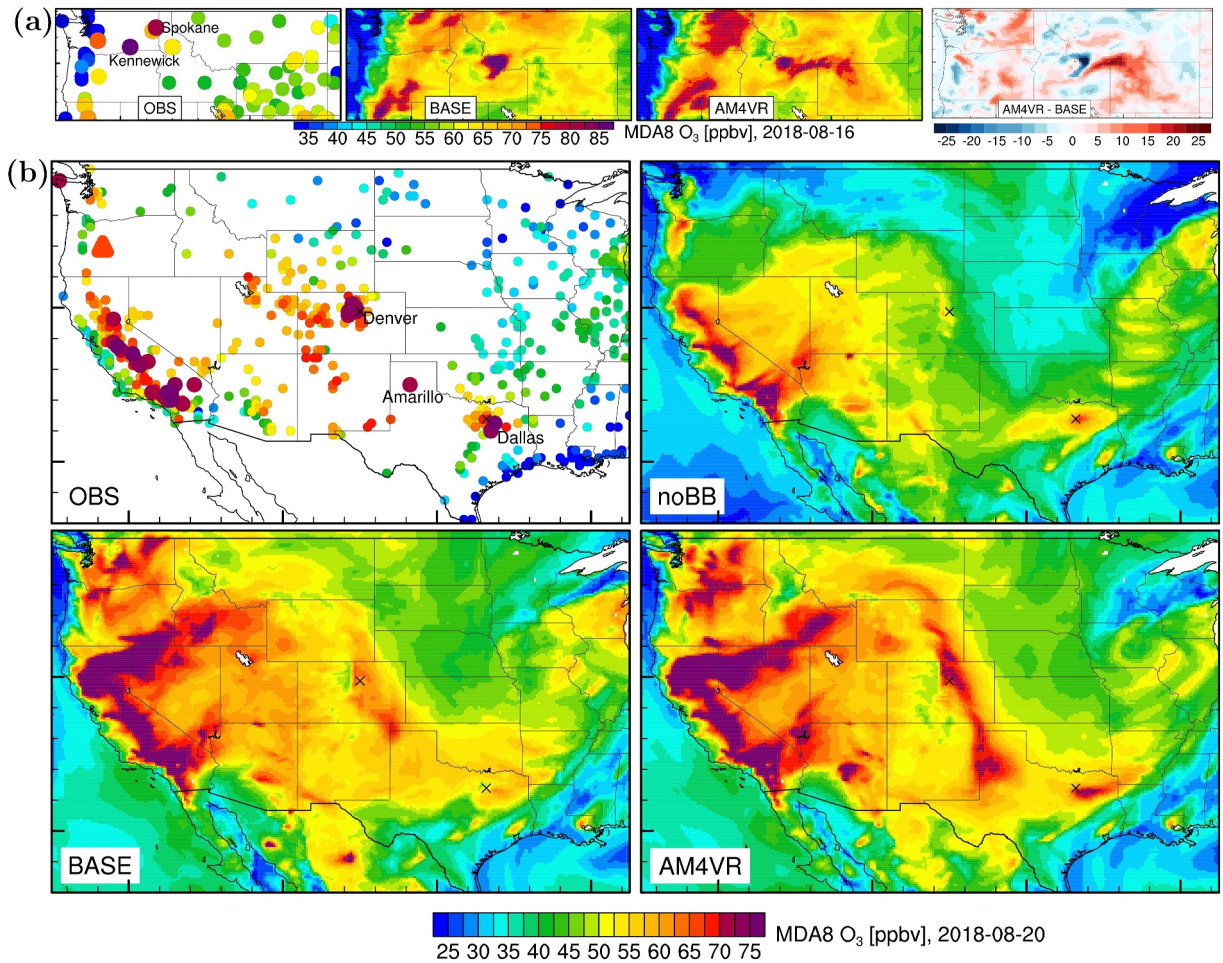

Figure 4. Maps of surface MDA8 O_3 on 16 and 20 August from observations (OBS) and model simulations with Biomass burning (BB) emitting NO_y as 100% NO (BASE), and with the NO_y partitioning (AM4VR). Also shown is the difference between AM4VR and BASE for 16 August and simulated O_3 with BB emissions of all NO_y and volatile organic compounds (VOCs) zero out (noBB) for 20 August.

with IMPROVE observations showing little OA enhancement at Wichita Mountain on 24 August (Figure 1f). California's Central Coast and San Joaquin Valley were also influenced by transported smoke on 24 August, with more sites exceeding 70 ppbv MDA8 O_3 on the smoky day (Figure S7 in Supporting Information S1).

6. Conclusions

Using observations and a new variable-resolution global model (Lin et al., 2024), we highlight the role of pyrogenic VOCs and NO_y evolution on O_3 production in smoke plumes. Rapid conversion of NO_x to NO_3^- and PAN reduces excessive O_3 production simulated in near-fire smoke plumes. When aged smoke plumes travel thousands of kilometers southward from Canada toward US cities, PAN thermally decomposes and thus enhances O_3 production. We identify the smoke-impacted days in US cities with observed MDA8 O_3 of 70–88 ppbv. The enhancement due to wildfire smoke ranges from 5 to 25 ppbv. For small cities like Kennewick and Boulder, O_3 produced during smoke transport is the main driver of O_3 increases and the NO_y parameterization can enhance in-plume O_3 production by 20%–45%. For larger cities like Denver and Dallas, O_3 is enhanced by production during smoke transport plus the in-situ production from mixing of smoke VOCs with urban NO_x. As large wildfires are projected to increase in western North America due to climate warming (Xie et al., 2022), accurate representation of VOCs and NO_y evolution in smoke is critical to assess the implications for US O_3 air quality.

10.1029/2024GL109369

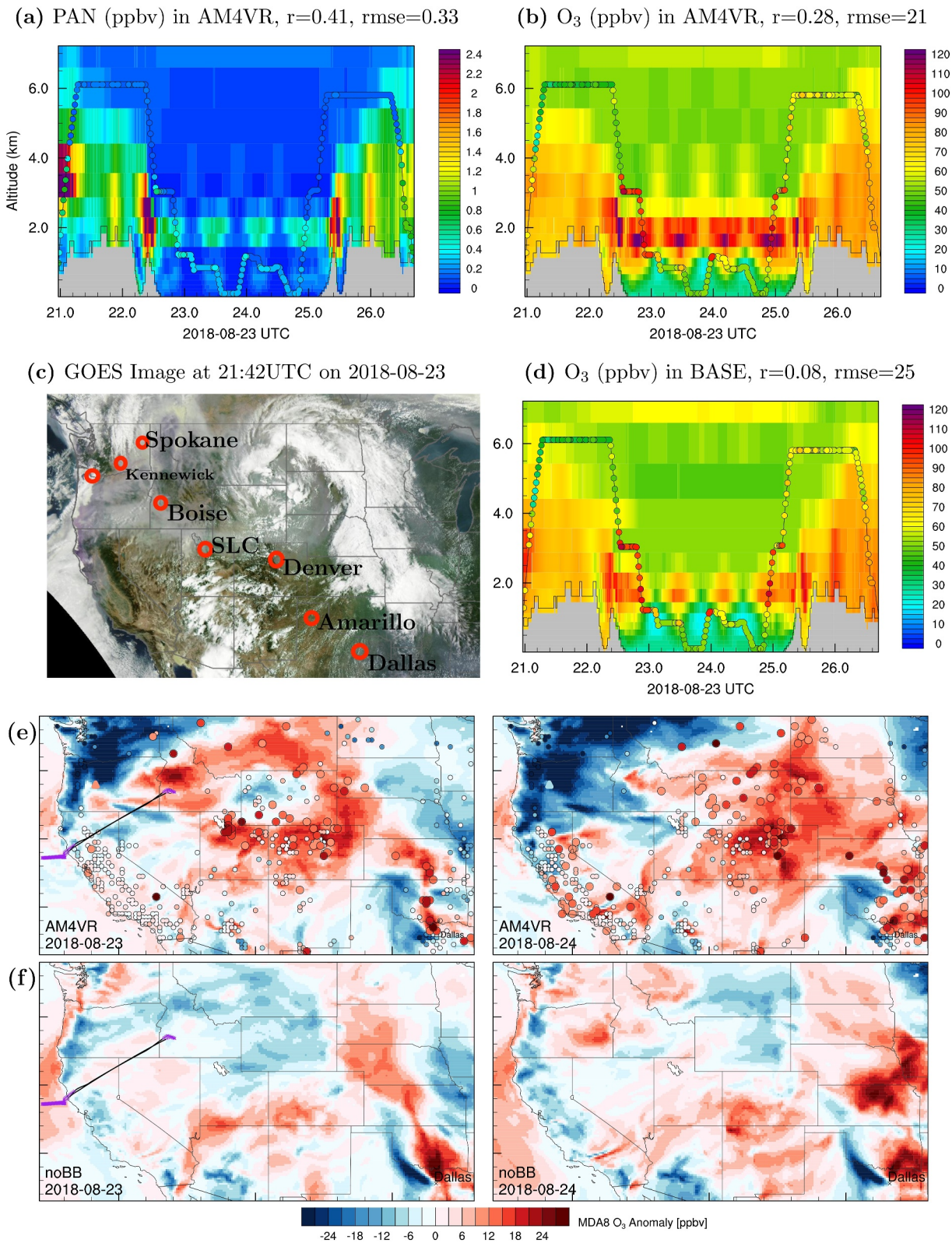

Figure 5. (a, b) Observed (circles) and AM4VR simulated peroxyacetyl nitrate (PAN) and O_3 for the 23 August flight; (c) GOES natural-color image; (d) O_3 from BASE; (e) maps of observed and simulated surface MDA8 O_3 anomalies on 23 and 24 August (relative to 22 August); (f) same as (e) but showing noBB results. The flight track between Idaho and California is shown (purple for below 4 km altitude).

Data Availability Statement

Source code of AM4VR is available at Lin (2023). WE-CAN data is available at https://data.eol.ucar.edu/master_lists/generated/we-can/.

Acknowledgments
We thank Songmiao Fan, Emily Fischer, Frank Flocke, Daniel A. Jaffe and Rui Wang for helpful comments. Funding for the WE-CAN data collection was provided by the US National Science Foundation (NSF award numbers: AGS-1650786, AGS-1650275, AGS-1950327, and AGS-1652688) and the US National Oceanic and Atmospheric Administration (NOAA) under award numbers NA17OAR4310010 and NA17OAR4310001. L.H. and W.P. were also supported by NSF Grants AGS-2144896 and EPSCoR-2242802.

References

Abatzoglou, J. T., & Williams, A. P. (2016). Impact of anthropogenic climate change on wildfire across western US forests. *Proceedings of the National Academy of Sciences of the United States of America*, *113*(42), 11770–11775. https://doi.org/10.1073/pnas.1607171113

Alvarado, M. J., Logan, J. A., Mao, J., Apel, E., Riemer, D., Blake, D., et al. (2010). Nitrogen oxides and PAN in plumes from boreal fires during ARCTAS-B and their impact on ozone: An integrated analysis of aircraft and satellite observations. *Atmospheric Chemistry and Physics*, *10*(20), 9739–9760. https://doi.org/10.5194/acp-10-9739-2010

Alvarado, M. J., Lonsdale, C. R., Yokelson, R. J., Akagi, S. K., Coe, H., Craven, J. S., et al. (2015). Investigating the links between ozone and organic aerosol chemistry in a biomass burning plume from a prescribed fire in California chaparral. *Atmospheric Chemistry and Physics*, *15*(12), 6667–6688. https://doi.org/10.5194/acp-15-6667-2015

Arnold, S. R., Emmons, L. K., Monks, S. A., Law, K. S., Ridley, D. A., Turquety, S., et al. (2015). Biomass burning influence on high-latitude tropospheric ozone and reactive nitrogen in summer 2008: A multi-model analysis based on POLMIP simulations. *Atmospheric Chemistry and Physics*, *15*(11), 6047–6068. https://doi.org/10.5194/acp-15-6047-2015

Baker, K. R., Woody, M. C., Tonnesen, G. S., Hutzell, W., Pye, H., Beaver, M., et al. (2016). Contribution of regional-scale fire events to ozone and $PM_{2.5}$ air quality estimated by photochemical modeling approaches. *Atmospheric Environment*, *140*, 539–554. https://doi.org/10.1016/j.atmosenv.2016.06.032

Baker, K. R., Woody, M. C., Valin, L., Szykman, J., Yates, E., Iraci, L., et al. (2018). Photochemical model evaluation of 2013 California wildfire air quality impacts using surface, aircraft, and satellite data. *Science of the Total Environment*, *637*, 1137–1149. https://doi.org/10.1016/j.scitotenv.2018.05.048

Bourgeois, I., Peischl, J., Neuman, J. A., Brown, S. S., Thompson, C. R., Aikin, K. C., et al. (2021). Large contribution of biomass burning emissions to ozone throughout the global remote troposphere. *Proceedings of the National Academy of Sciences of the United States of America*, *118*(52), e2109628118. https://doi.org/10.1073/pnas.2109628118

Brown, P. T., Hanley, H., Mahesh, A., Reed, C., Strenfel, S. J., Davis, S. J., et al. (2023). Climate warming increases extreme daily wildfire growth risk in California. *Nature*, *621*(7980), 760–766. https://doi.org/10.1038/s41586-023-06444-3

Cai, C. X., Kulkarni, S., Zhao, Z., Kaduwela, A. P., Avise, J. C., DaMassa, J. A., et al. (2016). Simulating reactive nitrogen, carbon monoxide, and ozone in California during ARCTAS-CARB 2008 with high wildfire activity. *Atmospheric Environment*, *128*, 28–44. https://doi.org/10.1016/j.atmosenv.2015.12.031

Cariolle, D., Caro, D., Paoli, R., Hauglustaine, D. A., Cuénot, B., Cozic, A., & Paugam, R. (2009). Parameterization of plume chemistry into large-scale atmospheric models: Application to aircraft NOx emissions. *Journal of Geophysical Research*, *114*(D19), D19302. https://doi.org/10.1029/2009jd011873

Coggon, M. M., Lim, C. Y., Koss, A. R., Sekimoto, K., Yuan, B., Gilman, J. B., et al. (2019). OH chemistry of non-methane organic gases (NMOGs) emitted from laboratory and ambient biomass burning smoke: Evaluating the influence of furans and oxygenated aromatics on ozone and secondary NMOG formation. *Atmospheric Chemistry and Physics*, *19*(23), 14875–14899. https://doi.org/10.5194/acp-19-14875-2019

Fiore, A. M., Fischer, E. V., Milly, G. P., Pandey Deolal, S., Wild, O., Jaffe, D. A., et al. (2018). Peroxy Acetyl Nitrate (PAN) measurements at northern midlatitude mountain sites in April: A constraint on continental source-receptor relationships. *Atmospheric Chemistry and Physics*, *18*(20), 15345–15361. https://doi.org/10.5194/acp-18-15345-2018

Fiore, A. M., Oberman, J. T., Lin, M. Y., Zhang, L., Clifton, O., Jacob, D., et al. (2014). Estimating North American background ozone in U.S. surface air with two independent global models: Variability, uncertainties, and recommendations. *Atmospheric Environment*, *96*, 284–300. https://doi.org/10.1016/j.atmosenv.2014.07.045

Fischer, E. V., Jacob, D. J., Yantosca, R. M., Sulprizio, M. P., Millet, D. B., Mao, J., et al. (2014). Atmospheric Peroxyacetyl Nitrate (PAN): A global budget and source attribution. *Atmospheric Chemistry and Physics*, *14*(5), 2679–2698. https://doi.org/10.5194/acp-14-2679-2014

Fountoukis, C., & Nenes, A. (2007). ISORROPIA II: A computationally efficient thermodynamic equilibrium model for K^+–Ca^{2+}–Mg^{2+}–NH^{4+}–Na^+–SO_4^{2-}–NO^{3-}–Cl^-–H_2O aerosols. *Atmospheric Chemistry and Physics*, *7*(17), 4639–4659. https://doi.org/10.5194/acp-7-4639-2007

Garofalo, L. A., Pothier, M. A., Levin, E. J. T., Campos, T., Kreidenweis, S. M., & Farmer, D. K. (2019). Emission and evolution of submicron organic aerosol in smoke from wildfires in the Western United States. *ACS Earth and Space Chemistry*, *3*(7), 1237–1247. https://doi.org/10.1021/acsearthspacechem.9b00125

Hagmann, R. K., Hessburg, P. F., Prichard, S. J., Povak, N. A., Brown, P. M., Fulé, P. Z., et al. (2021). Evidence for widespread changes in the structure, composition, and fire regimes of western North American forests. *Ecological Applications*, *31*(8), e02431. https://doi.org/10.1002/eap.2431

Hatch, L. E., Yokelson, R. J., Stockwell, C. E., Veres, P. R., Simpson, I. J., Blake, D. R., et al. (2017). Multi-instrument comparison and compilation of non-methane organic gas emissions from biomass burning and implications for smoke-derived secondary organic aerosol precursors. *Atmospheric Chemistry and Physics*, *17*(2), 1471–1489. https://doi.org/10.5194/acp-17-1471-2017

Jacob, D. (1999). *Introduction to atmospheric chemistry* (pp. 212–215). Princeton University Press.

Jaffe, D. A., O'Neill, S. M., Larkin, N. K., Holder, A. L., Peterson, D. L., Halofsky, J. E., & Rappold, A. G. (2020). Wildfire and prescribed burning impacts on air quality in the United States. *Journal of the Air & Waste Management Association*, *70*(6), 583–615. https://doi.org/10.1080/10962247.2020.1749731

Jaffe, D. A., & Wigder, N. L. (2012). Ozone production from wildfires: A critical review. *Atmospheric Environment*, *51*, 1–10. https://doi.org/10.1016/j.atmosenv.2011.11.063

Jin, L., Permar, W., Selimovic, V., Ketcherside, D., Yokelson, R. J., Hornbrook, R. S., et al. (2023). Constraining emissions of volatile organic compounds from western US wildfires with WE-CAN and FIREX-AQ airborne observations. *Atmospheric Chemistry and Physics*, *23*(10), 5969–5991. https://doi.org/10.5194/acp-23-5969-2023

Jin, X., Fiore, A. M., & Cohen, R. C. (2023). Space-based observations of ozone precursors within California wildfire plumes and the impacts on ozone-NOx-VOC chemistry. *Environmental Science & Technology*, *57*(39), 14648–14660. https://doi.org/10.1021/acs.est.3c04411

Juncosa Calahorrano, J. F., Lindaas, J., O'Dell, K., Palm, B. B., Peng, Q., Flocke, F., et al. (2021). Daytime oxidized reactive nitrogen partitioning in western U.S. wildfire smoke plumes. *Journal of Geophysical Research: Atmospheres*, *126*(4), e2020JD033484. https://doi.org/10.1029/2020JD033484

Langford, A. O., Senff, C. J., Alvarez, R. J., II., Aikin, K. C., Ahmadov, R., Angevine, W. M., et al. (2023). Were wildfires responsible for the unusually high surface ozone in Colorado during 2021? *Journal of Geophysical Research: Atmospheres*, *128*(12), e2022JD037700. https://doi.org/10.1029/2022JD037700

Liang, Y., Stamatis, C., Fortner, E. C., Wernis, R. A., Van Rooy, P., Majluf, F., et al. (2022). Emissions of organic compounds from western US wildfires and their near-fire transformations. *Atmospheric Chemistry and Physics*, *22*(15), 9877–9893. https://doi.org/10.5194/acp-22-9877-2022

Lin, M. (2023). Source code of AM4VR [Software]. *Zenodo*. https://doi.org/10.5281/zenodo.10257866

Lin, M., Holloway, T., Carmichael, G. R., & Fiore, A. M. (2010). Quantifying pollution inflow and outflow over East Asia in spring with regional and global models. *Atmospheric Chemistry and Physics*, *10*(9), 4221–4239. https://doi.org/10.5194/acp-10-4221-2010

Lin, M., Horowitz, L. W., Payton, R., Fiore, A. M., & Tonnesen, G. (2017). US surface ozone trends and extremes over 1980–2014: Quantifying the roles of rising Asian emissions, domestic controls, wildfires, and climate. *Atmospheric Chemistry and Physics*, *17*(4), 2943–2970. https://doi.org/10.5194/acp-17-2943-2017

Lin, M., Horowitz, L. W., Xie, Y., Paulot, F., Malyshev, S., Shevliakova, E., et al. (2020). Vegetation feedbacks during drought exacerbate ozone air pollution extremes in Europe. *Nature Climate Change*, *10*(5), 444–451. https://doi.org/10.1038/s41558-020-0743-y

Lin, M., Horowitz, L. W., Zhao, M., Harris, L., Ginoux, P., Dunne, J. P., et al. (2024). The GFDL variable-resolution global chemistry-climate model for research at the Nexus of US climate and air quality extremes. *Journal of Advances in Modeling Earth Systems*, *16*(4), e2023MS003984. https://doi.org/10.1029/2023MS003984

Lindaas, J., Farmer, D. K., Pollack, I. B., Abeleira, A., Flocke, F., Roscioli, R., et al. (2017). The impact of aged wildfire smoke on atmospheric composition and ozone in the Colorado Front Range in summer 2015. *Atmospheric Chemistry and Physics*, *17*, 10691–10707. https://doi.org/10.5194/acp-17-10691-2017

Lindaas, J., Pollack, I. B., Calahorrano, J. J., O'Dell, K., Garofalo, L. A., Pothier, M. A., et al. (2021a). Empirical insights into the fate of ammonia in western U.S. wildfire smoke plumes. *Journal of Geophysical Research: Atmospheres*, *126*(11), e2020JD033730. https://doi.org/10.1029/2020JD033730

Lindaas, J., Pollack, I. B., Garofalo, L. A., Pothier, M. A., Farmer, D. K., Kreidenweis, S. M., et al. (2021b). Emissions of reactive nitrogen from Western U.S. wildfires during summer 2018. *Journal of Geophysical Research: Atmospheres*, *126*(2), e2020JD032657. https://doi.org/10.1029/2020JD032657

Liu, X., Zhang, Y., Huey, L. G., Yokelson, R. J., Wang, Y., Jimenez, J. L., et al. (2016). Agricultural fires in the southeastern US during SEAC(4)RS: Emissions of trace gases and particles and evolution of ozone, reactive nitrogen, and organic aerosol. *Journal of Geophysical Research: Atmospheres*, *121*(12), 7383–7414. https://doi.org/10.1002/2016jd025040

McClure, C. D., & Jaffe, D. A. (2018). Investigation of high ozone events due to wildfire smoke in an urban area. *Atmospheric Environment*, *194*(2018), 146–157. https://doi.org/10.1016/j.atmosenv.2018.09.021

O'Dell, K., Hornbrook, R., Permar, W., Levin, E. J. T., Garofalo, L. A., Apel, E. C., et al. (2020). Hazardous air pollutants in fresh and aged western U.S. wildfire smoke and implications for long-term exposure. *Environmental Science & Technology*, *54*(19), 11838–11847. https://doi.org/10.1021/acs.est.0c04497

Palm, B. B., Peng, Q., Hall, S. R., Ullmann, K., Campos, T. L., Weinheimer, A., et al. (2021). Spatially resolved photochemistry impacts emissions estimates in fresh wildfire plumes. *Geophysical Research Letters*, *48*(23), e2021GL095443. https://doi.org/10.1029/2021GL095443

Pan, K., & Faloona, I. C. (2022). The impacts of wildfires on ozone production and boundary layer dynamics in California's Central Valley. *Atmospheric Chemistry and Physics*, *22*(14), 9681–9702. https://doi.org/10.5194/acp-22-9681-2022

Parisien, M. A., Barber, Q. E., Bourbonnais, M. L., Daniels, L. D., Flannigan, M. D., Gray, R. W., et al. (2023). Abrupt, climate-induced increase in wildfires in British Columbia since the mid-2000s. *Communications Earth & Environment*, *4*(1), 309. https://doi.org/10.1038/s43247-023-00977-1

Permar, W., Jin, L., Peng, Q., O'Dell, K., Lill, E., Selimovic, V., et al. (2023). Atmospheric OH reactivity in the western United States determined from comprehensive gas-phase measurements during WE-CAN. *Environmental Science: Atmospheres*, *3*(1), 97–114. https://doi.org/10.1039/D2EA00063F

Permar, W., Wang, Q., Selimovic, V., Wielgasz, C., Yokelson, R. J., Hornbrook, R. S., et al. (2021). Emissions of trace organic gases from western U.S. wildfires based on WE-CAN aircraft measurements. *Journal of Geophysical Research: Atmospheres*, *126*(11), e2020JD033838. https://doi.org/10.1029/2020JD033838

Rickly, P. S., Coggon, M. M., Aikin, K. C., Alvarez, R. J., Baidar, S., Gilman, J. B., et al. (2023). Influence of wildfire on urban ozone: An observationally constrained box modeling study at a site in the Colorado front range. *Environmental Science & Technology*, *57*(3), 1257–1267. https://doi.org/10.1021/acs.est.2c06157

Singh, H. B., Cai, C., Kaduwela, A., Weinheimer, A., & Wisthaler, A. (2012). Interactions of fire emissions and urban pollution over California: Ozone formations and air quality simulations. *Atmospheric Environment*, *56*, 45–51. https://doi.org/10.1016/j.atmosenv.2012.03.046

Tang, W., Emmons, L. K., Buchholz, R. R., Wiedinmyer, C., Schwantes, R. H., He, C., et al. (2022). Effects of fire diurnal variation and plume rise on U.S. air quality during FIREX-AQ and WE-CAN based on the Multi-Scale Infrastructure for Chemistry and Aerosols (MUSICAv0). *Journal of Geophysical Research: Atmospheres*, *127*(16), e2022JD036650. https://doi.org/10.1029/2022JD036650

US EPA. (2024). 8-Hour ozone nonattainment areas for the 2015 National Ambient Air Quality Standards (NAAQS). Retrieved from https://www3.epa.gov/airquality/greenbook/map8hr_2015.html

Val Martin, M., Kahn, R., & Tosca, M. (2018). A global analysis of wildfire smoke injection heights derived from space-based multi-angle imaging. *Remote Sensing*, *10*(10), 1609. https://doi.org/10.3390/rs10101609

van der Werf, G. R., Randerson, J. T., Giglio, L., van Leeuwen, T. T., Chen, Y., Rogers, B. M., et al. (2017). Global fire emissions estimates during 1997–2016. *Earth System Science Data*, *9*(2), 697–720. Latest data for 1997-2023. https://doi.org/10.5194/essd-9-697-2017

Warneke, C., Schwarz, J. P., Dibb, J., Kalashnikova, O., Frost, G., Al-Saad, J., et al. (2023). Fire influence on regional to global environments and air quality (FIREX-AQ). *Journal of Geophysical Research: Atmospheres*, *128*(2), e2022JD037758. https://doi.org/10.1029/2022JD037758

Xie, Y., Lin, M., Decharme, B., Delire, C., Horowitz, L. W., Lawrence, D. M., et al. (2022). Tripling of western US particulate pollution from wildfires in a warming climate. *Proceedings of the National Academy of Sciences of the United States of America*, *119*(14), e2111372119. https://doi.org/10.1073/pnas.2111372119

Xie, Y., Lin, M., & Horowitz, L. W. (2020). Summer $PM_{2.5}$ pollution extremes caused by wildfires over the Western United States during 2017–2018. *Geophysical Research Letters*, *47*(16), e2020GL089429. https://doi.org/10.1029/2020GL089429

Xu, L., Crounse, J. D., Vasquez, K. T., Allen, H., Wennberg, P. O., Bourgeois, I., et al. (2021). Ozone chemistry in Western U.S. wildfire plumes. *Science Advances*, *7*(50), eabl3648. https://doi.org/10.1126/sciadv.abl3648

Ye, X., Arab, P., Ahmadov, R., James, E., Grell, G. A., Pierce, B., et al. (2021). Evaluation and intercomparison of wildfire smoke forecasts from multiple modeling systems for the 2019 Williams Flats fire. *Atmospheric Chemistry and Physics*, *21*(18), 14427–14469. https://doi.org/10.5194/acp-21-14427-2021

Zhang, L., Jacob, D. J., Yue, X., Downey, N. V., Wood, D. A., & Blewitt, D. (2014). Sources contributing to background surface ozone in the US Intermountain West. *Atmospheric Chemistry and Physics*, *14*(11), 5295–5309. https://doi.org/10.5194/acp-14-5295-2014

Zhang, L., Lin, M., Langford, A. O., Horowitz, L. W., Senff, C. J., Klovenski, E., et al. (2020). Characterizing sources of high surface ozone events in the southwestern US with intensive field measurements and two global models. *Atmospheric Chemistry and Physics*, *20*(17), 10379–10400. https://doi.org/10.5194/acp-20-10379-2020

References From the Supporting Information

Apel, E., Hornbrook, R., & Hills, A. (2020). *Trace Organic Gas Analyzer (TOGA) data*. Version 1.0. UCAR/NCAR - Earth Observing Laboratory. https://doi.org/10.26023/F2JA-5WE7-ZH01

Briggs, N. L., Jaffe, D. A., Gao, H. L., Hee, J. R., Baylon, P. M., Zhang, Q., et al. (2016). Particulate matter, ozone, and nitrogen species in aged wildfire plumes observed at the Mount Bachelor Observatory. *Aerosol and Air Quality Research*, *16*(12), 3075–3087. https://doi.org/10.4209/aaqr.2016.03.0120

Buysse, C. E., Kaulfus, A., Nair, U., & Jaffe, D. A. (2019). Relationships between particulate matter, ozone, and nitrogen oxides during urban smoke events in the western US. *Environmental Science & Technology*, *53*(21), 12519–12528. https://doi.org/10.1021/acs.est.9b05241

Campos, T. (2019). *Picarro G2401-m WS-CRDS CO_2, CH_4, CO and H_2O in situ mixing ratio observations - ICARTT format*. Version 1.2. UCAR/NCAR - Earth Observing Laboratory. https://doi.org/10.26023/NNYM-Z18J-PX0Q

Flocke, F., & Shertz, S. (2019). *PAN CIMS (Chemical Ionization Mass Spectrometer) data*. Version 1.0. UCAR/NCAR - Earth Observing Laboratory. https://doi.org/10.26023/FRAX-1G7V-DG0X

Lin, M., Fiore, A. M., Cooper, O. R., Horowitz, L. W., Langford, A. O., Levy, H., II, et al. (2012a). Springtime high surface ozone events over the western United States: Quantifying the role of stratospheric intrusions. *Journal of Geophysical Research*, *117*(D21), D00V22. https://doi.org/10.1029/2012JD018151

Lin, M., Fiore, A. M., Horowitz, L. W., Cooper, O. R., Naik, V., Holloway, J., et al. (2012b). Transport of Asian ozone pollution into surface air over the western United States in spring. *Journal of Geophysical Research*, *117*(D21), D00V07. https://doi.org/10.1029/2011JD016961

Ninneman, M., & Jaffe, D. A. (2021). The impact of wildfire smoke on ozone production in an urban area: Insights from field observations and photochemical box modeling. *Atmospheric Environment*, *267*, 118764. https://doi.org/10.1016/j.atmosenv.2021.118764

Weinheimer, A., Montzka, D., & Tyndall, G. (2019). *Chemiluminescence instrument for NO, NO_2, and O_3 data*. Version 1.0. UCAR/NCAR - Earth Observing Laboratory. https://doi.org/10.26023/EW3Y-4S35-790B

Yokelson, R. J., Crounse, J. D., DeCarlo, P. F., Karl, T., Urbanski, S., Atlas, E., et al. (2009). Emissions from biomass burning in the Yucatan. *Atmospheric Chemistry and Physics*, *9*(15), 5785–8512. https://doi.org/10.5194/acp-9-5785-2009